JOM, Vol. 72, No. 2, 2020
https://doi.org/10.1007/s11837-019-03930-w

Fabrication of a Cu/TiNi Composite with High Air-Tightness and Low Thermal Expansion

TAO XIAO,[1,2] ZHOU LI,[1,2] ZHU XIAO,[1] XI ZHANG,[1] WENTING QIU,[1] YANG WANG,[1] XIAOLI GUO,[1] and QIAN LEI [1,3,4]

1.—State Key Laboratory for Powder Metallurgy, Central South University, Changsha 410083, China. 2.—School of Materials Science and Engineering, Central South University, Changsha 410083, China. 3.—Department of Materials Science and Engineering, College of Engineering, University of Michigan, Ann Arbor 48109, USA. 4.—e-mail: leiqian@csu.edu.cn

Copper alloys exhibit a positive thermal expansion effect, which is undesirable to materials as in service, while TiNi composite materials exhibit negative thermal expansion. In this study, we fabricated a new high-density Cu/TiNi composite with low thermal expansion through electroless deposition and powder metallurgy. Mixed powders of 15% electroless deposited Cu-TiNi composite powders, and 85% prepared Cu powders were cold extruded, vacuum hot press heat-treated, and hot compressed at 900°C for 2 h. The coefficients of thermal expansion of the Cu/TiNi composite at 100°C, 200°C, and 300°C were 13.99×10^{-6}/K, 17.28×10^{-6}/K, and 17.72×10^{-6}/K, respectively. The fabricated Cu/TiNi composite materials showed good air-tightness and negative thermal expansion, so have bright prospects in lead frames and other electrical and electronic applications.

INTRODUCTION

The ideal electronic packaging materials should have the following properties: low density, high thermal conductivity, adjustable thermal expansion coefficient, high compactness, and non-leakage. SiC_p/Al, Cu/Mo, and Cu/W alloys have been used to make electronic packaging materials.[1–3] The thermal conductivity and expansion coefficient are controllable by changing the content of W in the Cu/W alloy,[4] and the content of Mo in the Cu/Mo alloy.[5] However, the interface bonding strength of Cu/Mo and Cu/W packaging materials is low since the Mo and W are insoluble with Cu.[6] Besides, the residual carbon impurity in the Cu/Mo and Cu/W materials leads to cavities and decreases the thermal conductivity.[7] Copper and carbon are immiscible in the melt. Thus, cavities formed and severely affected the thermal conductivity and air-tightness of Cu/Mo and Cu/W materials. Moreover, the content of Mo and W should be high enough to obtain a low thermal expansion coefficient. The densities of Cu/Mo and Cu/W materials are high because of the high densities of Mo and W, limiting their application.

There is an effective method of fabricating low expansion coefficient materials through stacking Cu matrix and negative thermal expansion materials.[8,9] Adjusting the volume fraction of the negative expansion materials (NTEM) in the composites would give the thermal expansion coefficient. The air-tightness loss of the Cu/NTEM composites is small.[10] The common NTEMs are ZrW_2O_8, $Zr_2(WO_4)(PO_4)_2$, ZrV_2O_7, and other compounds, which are difficult to process and deform.[11–13] However, these negative thermal expansion materials will diffuse, and interfacial reactions with Cu result in loss of the negative thermal expansion materials. Verdon et al. cold compressed the mixed powders of 67 vol.% Cu and 33 vol.% ZrW_2O_8 at a pressure of 300 MPa, and then hot compressed at a pressure of 103 MPa at 600°C with a dwell time of 3 h. Unexpectedly, the ZrW_2O_8 has been composited and transferred to WO_3 and other multivariate compounds. Then the expansion coefficient of the materials is increased.[14]

Recent investigations have proved that the TiNi shape memory alloys present a thermal expansion of approximately -21 to -8×10^{-6}/°C.[15] After pretreatment of TiNi alloy with different processes,

(Published online December 6, 2019)

the coefficient of thermal expansion in the range of 25–100°C was approximately -8 to -21×10^{-6}/°C. A small number of TiNi materials could decrease the thermal expansion coefficient of Cu/TiNi composites, and high air-tightness can be approached.[16,17] Hot roll bonding is a method of bonding a heat-treated Cu plate and a TiNi plate into one composite plate through rolling. The interface strength of the Cu/TiNi composite plate is low or missing because of interface oxidization. The shape of the Cu/TiNi composite plate is difficult to control due to the difference in the deformation resistances from the Cu plate and the TiNi plate. The use of powder metallurgy to fabricate a uniform Cu/TiNi composite could avoid the above problem. However, high residual stress was detected on the samples directly after sintering and cooling down to room temperature because of the vast difference in the thermal expansion coefficients of Cu powders and TiNi powders. The residual thermal stress stored in the composite will lead to cracking, and a decrease in air-tightness.

An electroless copper depositing technology was employed to enhance the surface of the TiNi powders, and improve the bonding strength. Then hot extrusion was used to fabricate Cu/TiNi composites with low density, high gas tightness, and low thermal expansion coefficient.

EXPERIMENTAL PROCEDURES

The chemical composition of the studied shape memory alloy powders was Ti-53.40 at %Ni, with a powder size of 10–50 μm. The electroless deposition solution included an inorganic solution containing Cu^{2+}, glyoxylic acid, a reductant, and a conditioning agent. The Cu-based inorganic solution included $CuSO_4$, EDTA and KOH. $CuSO_4$ provided the copper ions. The EDTA is a reductant; acetaldehyde was employed to stabilize the surface of the Cu powders.[18] The inhibitor of reducing agent is KOH. The dipyridyl was employed to maintain the pH value at 10. The procedure for depositing Cu on the TiNi powder was as follows: firstly, the TiNi powders were transferred into a solution with water and $CuSO_4$ solution. The mixed solution contained TiNi, and the $CuSO_4$ was warmed at 40°C for 15 min. KOH, dipyridyl, and acetaldehyde were added into the warmed solution one after another, then the solution was stirred for 10 min. The temperatures for electroless depositing were 50°C, 60°C, 70°C, and 80°C, respectively. The reaction for depositing Cu on the surface of the TiNi powders finished in 30 min, and the color of the solution had completely changed by the end. The TiNi powders coated with Cu were dried at 80°C, and then they were annealed in a hydrogen annealing furnace. A lab blender was used to mix 15% Cu-TiNi composite powder and 85% Cu powder. The powders were cold extruded at first, then hot compressed in a vacuum hot pressing furnace at 900°C for 2 h, with an extrusion ratio of 10:1. Figure 1 shows the experimental procedure of the thermal compression process, and the as-received extruded samples had dimensions of ϕ 30 $\times$ 20 mm. A DIL 402 thermal dilatometer was employed to measure the thermal expansion coefficient of the extruded sample at designed environment temperatures of 25–300°C. The gas tightness of the machined extruded sample was measured with an air-tightness tester. The TiNi powders with Cu shells and the extruded samples were mounted, polished, and characterized using a Leica C.E. optical microscope, a Sirion 200 scanning electron microscope, and a Genesis 60S EDX. An x-ray diffraction test was employed to determine the phases in the as-received Cu and TiNi powders, the Cu-TiNi composite powders, and the extruded Cu/TiNi sample.

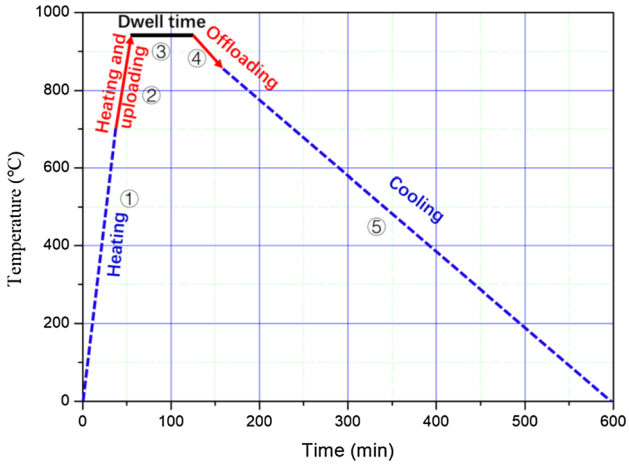

Fig. 1. Experimental procedure for the thermal compression process. (1) Heating to 700°C with a heating rate of 10°C/min; (2) heating to 950°C with a heating rate of 7.5°C/min; (3) loading on the Cu and Cu-TiNi powders at 950°C with a pressure of 20 MPa, the loading started at 700°C; (4) dwelling at 950°C for 60 min; (5) offloading; (6) extruded samples were cooled with hot compression equipment.

RESULTS AND DISCUSSION

Electroless Deposition Process

Figure 2 shows photomicrographs of as-received TiNi powders and Cu powders. The TiNi powders were spherical with an average radius of 10 μm, while the as-received Cu powders had irregular morphology. Figure 3 shows the microstructure of the surface of the TiNi powders after deposition of copper at different temperatures. The total volume of the mixture solution was 0.1 L, which included a solution with a concentration of 0.05 mol/L Cu^{2+}, 1.5 mL glyoxylic acid with a concentration of 9 mol/L, and 4.5 mL of KOH solution with a concentration of 10 mol/L. After deposition at 50°C, the Cu layer is nonuniform: only parts of the surface had Cu deposited on them (Fig. 3a). The Cu layer became more uniform and denser as the layer treatment

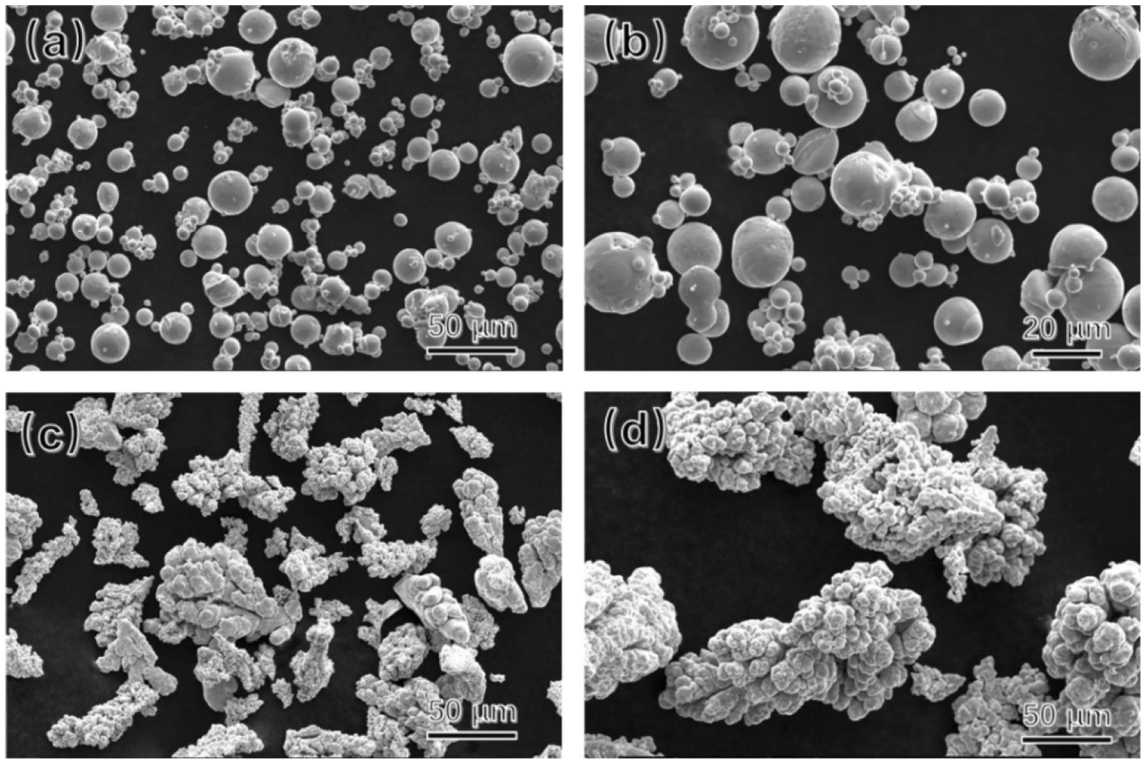

Fig. 2. Morphology of as-received TiNi and Cu powders. (a), (b) TiNi powders. (c), (d) Cu powders.

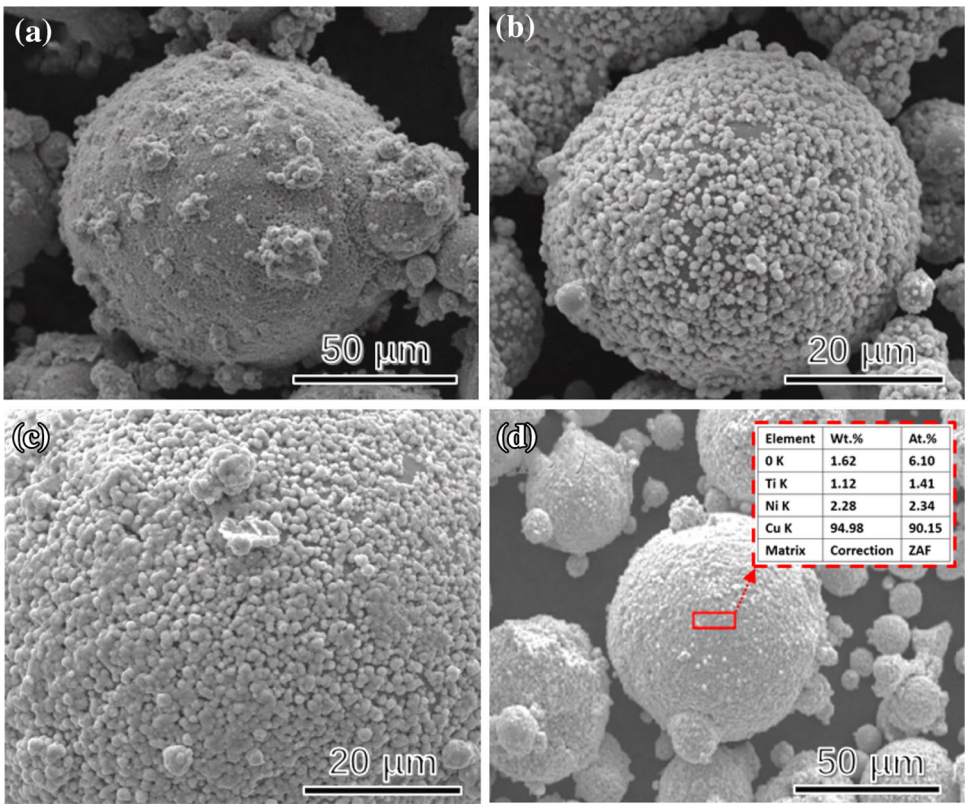

Fig. 3. Microstructure of the surface of the TiNi powders after coating with copper at different temperatures. (a) 50°C; (b) 60°C; (c) 70°C; (d) 80°C.

temperature was increased to 60°C and 70°C, as shown in Fig. 3b and c. Oxygen was detected in the Cu layer when the deposition treatment temperature was increased to 80°C, as shown in Fig. 3d. Figure 4 shows the surface of the TiNi powders after depositing the copper layer in a mixture solution with different dipyridyl concentrations (20–40 mg/L). The coated Cu layer is much denser and more uniform than the previous ones, as shown in Fig. 4c. Figure 5 gives the microstructure and element line analysis of the TiNi powders coated at a dipyridyl concentration of 30 mg/L. The section view of the powder presents a core-shell structure, with a Cu shell and TiNi core. After the addition of pyridine, the Cu layer is closer and more uniform. For a single particle, the matrix phase is light gray and the Cu layer is white. Cu is evenly distributed on the surface of the TiNi powder. The thickness of the deposition layer is about 2 μm.

TiNi-Cu/Cu Composites

We analyzed the microstructure of TiNi-Cu/Cu composites after the molding process. The Cu/TiNi composite powders were mixed with pure Cu powder at a volume ratio of 15:85. The actual weight ratio was W_{Cu}:W_{TiNi} = 25:1. The x-ray diffraction patterns of the mixed as-received Cu and compressed Cu/TiNi powders are shown in Fig. 6. After cold extrusion and vacuum hot pressing at 900°C for 2 h, the mixed powders were coated with a pure copper belt. Thermal extrusion was carried out at 900°C, with an extrusion ratio of 10:1. The microstructure of the thermal compressed sample and the element distribution in TiNi powders coated with Cu are shown in Fig. 7. The TiNi powders were distributed in the Cu matrix. Figure 7b shows the elemental line distribution of the alloy after vacuum hot pressing at 900°C for 2 h, while the balls of Cu/TiNi composites are ellipsoid. The interface element line in Fig. 7b shows that there are some diffused Ti and Ni elements in the copper layer that coats the Cu/TiNi composite powder. Typical SEM images of pressurized bar cross-sections show that Cu/TiNi composite particles still maintain their nuclear/shell structure. The composite powder has promoted the combination of Cu/TiNi composite particles and copper matrix after vacuum hot pressing and hot extrusion (Fig. 7b). The distribution of elemental lines in Fig. 7c indicates that there is a significant diffusion of Ti and Ni elements in the copper coating layer of the Cu/TiNi composite powders.

Air-Tightness and Thermal Expansion Coefficient

After hot extrusion, the sample's leakage rates were measured. The atmospheric pressure was 3.6×10^{-6} Pa in the initial state, and it is only 26.3×10^{-6} Pa after 1500 h, as shown in Fig. 8a. The compressed sample shows good air-tightness. Figure 8b shows the thermal expansivity variation with the temperature. The coefficient of thermal

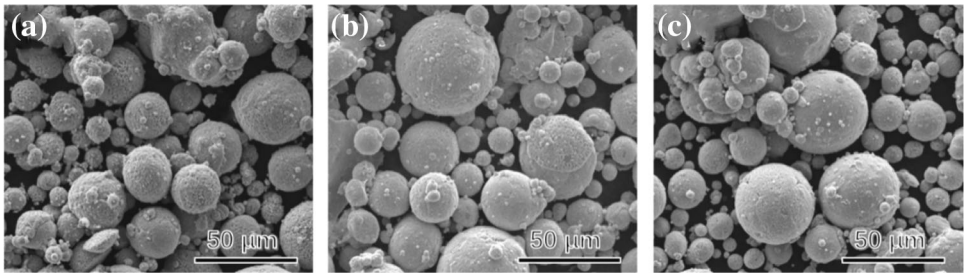

Fig. 4. Microstructure of the TiNi powders coated at different dipyridyl concentrations: (a) 20 mg/L; (b) 30 mg/L; (c) 40 mg/L.

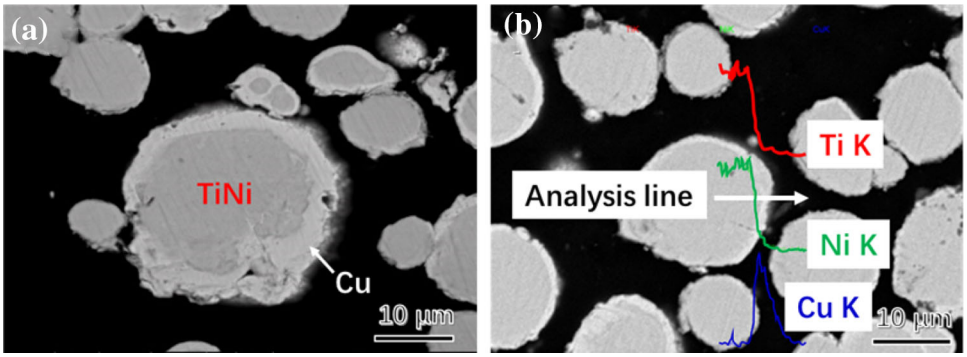

Fig. 5. Microstructure and element distribution of TiNi powders coated at a dipyridyl concentration of 30 mg/L. (a) cross-section; (b) element line analysis of Ti, Ni, and Cu.

expansion (CTE) of Cu is 17.79 × 10^{-6}/K, while the fabricated Cu/TiNi composite showed low thermal expansion. The CTEs of the Cu/TiNi composite are 13.99 × 10^{-6}/K, 17.28 × 10^{-6}/K, and 17.72 × 10^{-6}/K at 100°C, 200°C, and 300°C, respectively.

The thermal expansion behavior, caused by the change in atomic thermal vibration in the lattice, is

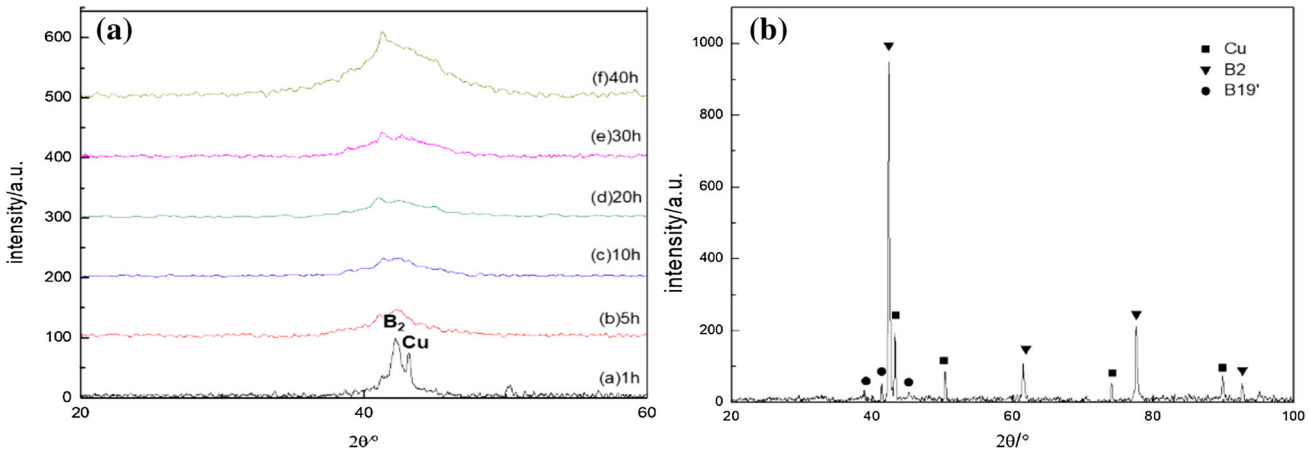

Fig. 6. X-ray diffraction pattern of the mixed as-received Cu (a) and mixed Cu/TiNi powders (b).

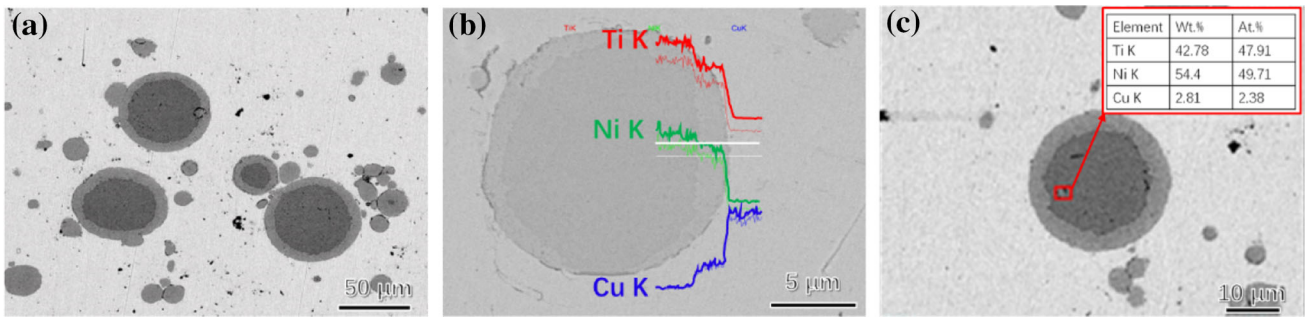

Fig. 7. Microstructure of the thermal compressed sample and the element distribution in TiNi powder coated with Cu. (a) Powder distribution; (b) element line analysis of Ti, Ni, and Cu in Cu/TiNi compressed samples; (c) element distribution of the core of TiNi powders coated with Cu.

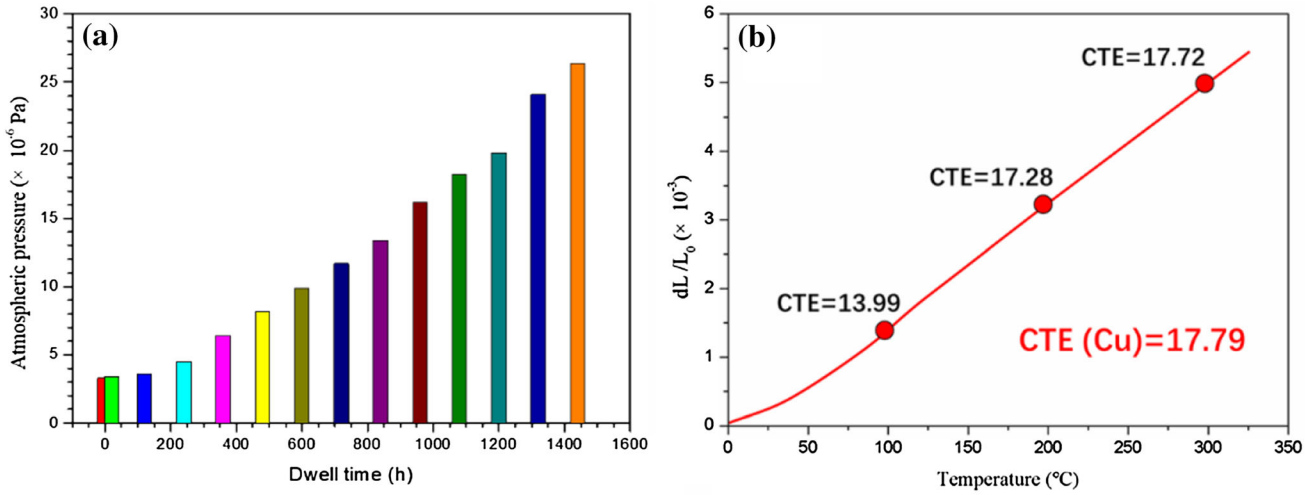

Fig. 8. Properties analysis: (a) atmospheric pressure variation with the dwell time in the air-tightness test; (b) thermal expansivity variation with temperature.

due to temperature rise. It occurs during heating, and the B19′ → B2 phase change occurs when the temperature reaches the austenite transition temperature in TiNi alloy. The austenite phase volume is smaller than the martensite phase in TiNi alloy. The composite material exhibits good volume shrinkage at the macroscopic level. As the austenite transition and temperature A_f is reached, the material no longer causes volume shrinkage, due to the phase change. The samples go back to positive thermal expansion. At this time, the B2 phase content in the TiNi alloy reaches its maximum. The volume expansion caused by the conventional thermal vibration of atoms in the lattice is smaller than the volume shrinkage caused by phase change. The volume shrinkage is still visible at the macroscopic level. The material appears to undergo normal thermal expansion when the temperature continues to rise. This leads to the end temperature for the NTEM behavior of the shrinking material, which lags behind the end temperature of the austenitic phase change. Another reason is the effect of the heat treatment process on the negative thermal expansion of TiNi alloy. Without enough stress aging treatment, the fraction of precipitated Ti_3Ni_4 is small. An active internal stress field formed, the specimen occurs normal thermal expansion and contraction. The samples are treated with aging under the applied constraint stress. The Ti_3Ni_4 phase is greatly precipitated, forming a valid internal stress field so that the TiNi alloy produces negative thermal expansion behavior.[19,20] The constraint temperature and time have a more significant influence on the negative thermal expansion behavior of TiNi alloy, and the effect of the constrained stress is relatively small.

CONCLUSION

New high-density Cu/TiNi composites with high air-tightness and low thermal expansion have been fabricated through Cu deposition and powder metallurgy. TiNi powders coated with a dipyridyl concentration of 30 mg/L and drying at 80°C show proper welding properties between the Cu deposition layer and the TiNi matrix. The Cu/TiNi composite materials were created by cold extrusion, vacuum hot pressing heat-treatment, and were hot-compressed at 900°C for 2 h. The CTEs of the Cu/TiNi composite at 100°C, 200°C, and 300°C were 13.99×10^{-6}/K, 17.28×10^{-6}/K, and 17.72×10^{-6}/K, respectively. The fabricated Cu/TiNi composites showed good air-tightness and low thermal expansion.

ACKNOWLEDGEMENTS

This work was supported by the National MCF Energy R&D Program of China (2018YFE0306100), the National Natural Science Foundation of China (51901250), and the National Natural Science Foundation of Hunan Province (2019JJ50765).

REFERENCES

1. B. Derby, Y.C. Cui, J. Baldwin, R. Arroyave, M.J. Demkowicz, and A. Misra, *Mater. Res. Lett.* 7, 1 (2019).
2. Q. Zhang, G.H. Wu, L.T. Jiang, and B.F. Luan, *Compos. A.* 34, 1023 (2003).
3. Y. Nerthigan, A.K. Sharma, S. Pandey, and H.F. Wu, *Microchim. Acta* 186, 130 (2019).
4. G.S. Jiang, Z.F. Wang, and H. Wu, *Powder. Metall. Technol.* 25, 126 (2007).
5. Y.G. Chen and B.X. Liu, *J. Alloy. Compd.* 261, 217 (1997).
6. Th. Schubert, B. Trindade, T. Weißgarber, and B. Kieback, *Mater. Sci. Eng. A* 475, 39 (2008).
7. H.K. Kang and S.B. Kang, *Surf. Coat. Technol.* 182, 124 (2004).
8. J.G. Cheng, C.P. Lei, E.T. Xiong, Y. Jiang, and Y.H. Xia, *J. Alloy. Compd.* 421, 146 (2006).
9. M. Rosinski, E. Fortuna, A. Michalski, Z. Pakiela, and K.J. Kurzydlowski, *Fusion Eng. Des.* 82, 2621 (2007).
10. J.F. Li, Z.Q. Zheng, X.W. Li, and Z.W. Peng, *Mater. Des.* 30, 314 (2009).
11. H. Holzer and D.C. Dunand, *J. Mater. Res.* 14, 780 (1999).
12. M. Cetinkol, A.P. Wilkinson, and C. Lind, *Phys. Rev. B* 79, 224118 (2009).
13. J.S.O. Evans, *J. Chem. Soc. Dalton Trans.* 1, 3317 (1999).
14. X.W. Li, Z.Q. Zheng, J.F. Li, S.C. Li, and X.Y. Wei, *Rare Met. Mater. Eng.* 36, 879 (2007).
15. K.A. Jafar, D. Antonin, and E. Gunther, *Acta Mater.* 50, 4255 (2002).
16. V. Kolomytsev, V. Nemoshkalenko, YuN Koval, A. Kozlov, B. Mordyuk, G. Prokopenko, P. Ochin, and R. Portier, *J. de Phys. IV (Proceedings)* 112, 1159 (2003).
17. S. Hao, L. Cui, Z. Chen, D. Jiang, Y. Shao, J. Jiang, M. Du, Y. Wang, D.E. Brown, and Y. Ren, *Adv. Mater.* 25, 1199 (2013).
18. S.S. Joshi, S.F. Patil, V. Iyer, and S. Mahumuni, *Nanostruct. Mater.* 10, 1135 (1998).
19. X.J. Yan, D.Z. Yang, and X.P. Liu, *Mater. Charact.* 58, 262 (2007).
20. B.Y. Li, L.J. Rong, and Y.Y. Li, *J. Mater. Res.* 13, 2847 (1998).